International Journal on
"Technical and Physical Problems of Engineering"
(IJTPE)
Published by International Organization of IOTPE

ISSN 2077-3528
IJTPE Journal
www.iotpe.com
ijtpe@iotpe.com

March 2019 | Issue 38 | Volume 11 | Number 1 | Pages 1-9

SENSORLESS SPEED CONTROL OF A BLDC MOTOR USING IMPROVED SLIDING MODE OBSERVER TECHNIQUE

M. Topal [1] I. Iskender [2] N. Genc [3]

1. Department of Electrical and Electronics Engineering, Gazi University, Ankara, Turkey, mustafa.topal@tubitak.gov.tr
2. Department of Electrical and Electronics Engineering, Cankaya University, Ankara, Turkey, ires@cankaya.edu.tr
3. Department of Electrical and Electronics Engineering, Van Yuzuncu Yil University, Van, Turkey, nacigenc@.yyu.edu.tr

Abstract- This paper proposes controlling the velocity of BLDC motor using sliding mode observer technique based on the estimation of back electromotive force (back EMF). There are many different sensorless control methods for BLDC motor, but in this paper one of them is examined in detail, comparing with the zero crossing points detection of back EMF and hall sensor control. The proposed method estimates the velocity and rotor position by measuring terminal voltages and currents. According to the rotor position, two inverter switches are energized to commutate the phases of BLDC motor. As comparing desired and real line currents, the commutation signals are acquired with hysteresis band. The simulation model of the suggested method is performed by using MATLAB Simulink environment and results have been simulated to interrogate the performance of the BLDC motor under a load change condition also with reference speed.

Keywords: BLDC Motor, Back Electromotive Force (Back EMF), Zero Crossing Points (ZCP), Sliding Mode Observer (SMO), Hall Sensor.

I. INTRODUCTION

Nowadays, electricity is one of the most needed and important energy sources. It is utilized in almost all areas of industry, military, aerospace and our daily life for a long time. The motors which are used in one of these areas are the heart of industrial systems because of that they have been using as electromecanical energy conversion device for many years. To satisfy the demands for various implements, different types of motors have been designed. One of these motors is BLDC motor which gradually is gaining popularity on account of its high performance, low repairing cost, small volume and high torque. Moreover, BLDC motor can run over broad bounds of speeds while the commutation features of a brushed type dc motor limit its speed range. BLDC motor, with its trapezoidal back EMF form, needs six different rotor position data to run because of no commutators or brushes. The rotor position signals are typically generated with Hall effect sensors or encoders put in the motor. Nevertheless, these sensors have some disadvantages such as increasing the cost and needing particular layout for mounting.

Additionally, these sensors are sensitive to temperature, thus the running of the motor is limited. The reliability of the system could decrease on account of the additional components and wiring [1]. They also increase the motor size and require elaborate regulation to be mounted [2]. Because of these drawbacks, engineers have been working to remove the disadvantages of regarding position sensors and improve all of the system. For these reasons many sensorless methods have been developed and most of them are still using at many applications.

The BLDC motor applications where position sensors are not used attract great interest in the industry world. A lot of sensorless methods for the BLDC motor are existing in literature like, the detection of zero crossing points for back-EMF [3], the detection of voltage component of third harmonic [4], the integration method of back-EMF [5], the detection of the frewheeling diodes conduction periods [6], estimation by observer [7].

Back EMF estimation methods is typically based on the determination of the back EMF zero crossing points. Back EMF estimation technique is done by measuring the terminal voltages according to a virtual neutral point as is proposed in [8]. Low pass filters are utilized to eliminate the higher harmonics, and hence a delay has been occured in the measured terminal because of filtering, which also limits the operating speed. Using this method is conveinent for restricted speed range.

The method of detection of the third harmonic component is quite relevant method for back EMF determination and is proposed in [4]. Although this method presents wider speed range and small phase delay comparing with the terminal voltage measuring method, the integration process may cause noise and offset errror at low speed.

Back EMF integration method of the idle phase for the commutation is proposed in [5]. Integration process begins with sensing the zero crossing point and finishes with detecting the treshold value, which shows commutation instants. The performance of this technique is poor at low speed.

With regard to the free-wheeling diode conduction method, back EMF zero crossing points are determined in open phase with sensing terminal current [6]. This method

has good performance both at higher and lower speeds. However, this technique needs six additional power supplies because of sensing the currents which flow through free-wheeling diodes.

In [7], an observer which estimates the back EMF from mathematical calculations presents rotor position information using its calculations. It has quite high performance and does not require any circuits.

In this paper, three different methods have been applied to control velocity of the motor and these methods are hall sensor, direct back EMF detection from terminal voltages and sliding mode observer techniques. Each techniques is individually simulated and analysed on the Matlab Simulink platform. The basic opinion of this paper is to control velocity of the BLDC motor by using three different methods.

The paper organization is as follows; in Section II the operating principle of the BLDC motors is presented. In Section III the proposed three methods are used to control velocity with sensor and sensorless techniques. In Section IV the methods are simulated and compared with each other. Conclusions and discussions are presented in the last section.

II. OPERATION PRINCIPLE OF BLDC MOTORS

Typically, BLDC motor with its three phase windings on stator is energized by a three phase inverter including six semiconductor switches and diodes. Figure 1 denotes BLDC motor equivalent circuit and Figure 2 shows the motor drive systems with using the hall sensor which gives rotor position information to trigger Gates of the inverter.

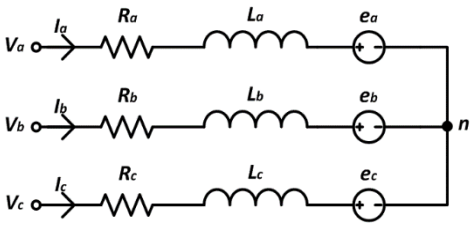

Figure 1. BLDC motor equivalent circuit

It is considered that all resistance and inductance of the windings are equal to each other and stated as R_s and L_s respectively, the phase "A" terminal voltage according to the star point V_{an}, is given in (1);

$$V_{an} = I_a R_a + L_a \frac{dI_a}{dt} + e_{an} \tag{1}$$

where, R_a is stator resistance, L_a is phase inductance, e_{an} is back EMF, and I_a is current of the phase "A". Similarly, this equation can be written again for the other two phases, indicated in (2) and (3);

$$V_{bn} = I_b R_b + L_b \frac{dI_b}{dt} + e_{bn} \tag{2}$$

$$V_{cn} = I_c R_c + L_c \frac{dI_c}{dt} + e_{cn} \tag{3}$$

The above equations can be combined in matrix form as in (4);

$$\begin{bmatrix} V_a \\ V_b \\ V_c \end{bmatrix} = \begin{bmatrix} R_s & 0 & 0 \\ 0 & R_s & 0 \\ 0 & 0 & R_s \end{bmatrix} \begin{bmatrix} I_a \\ I_b \\ I_c \end{bmatrix} + \begin{bmatrix} L_s & 0 & 0 \\ 0 & L_s & 0 \\ 0 & 0 & L_s \end{bmatrix} \frac{d}{dt} \begin{bmatrix} I_a \\ I_b \\ I_c \end{bmatrix} + \begin{bmatrix} e_a \\ e_b \\ e_c \end{bmatrix} \tag{4}$$

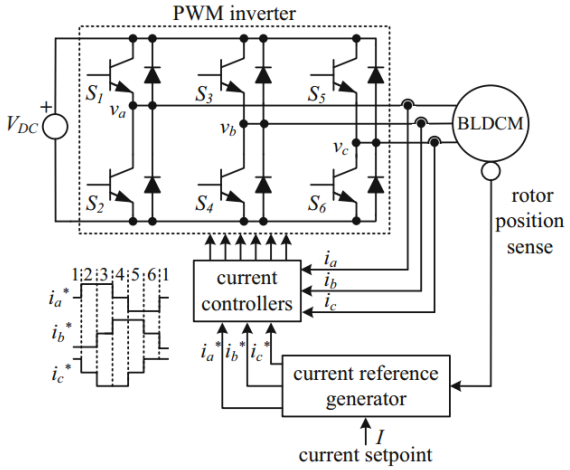

Figure 2. BLDC motor and drive systems [9]

In order to drive the motor, each phase current flows through inverter with respect to the rotor position ensured by sensor or sensorless techiques. As a result of this, the motor begins to rotate according to commutation steps. At any time, the two phases are excited throughout 120° interval while the third phase is floating. At each commutation step, one of two conducting windings is positive, other is negative and also there is a non-energized phase [10]. Due to existing an interaction between stator coil and rotor magnetic field is generated and thus torque is produced. Theoretically, peak torque happens when the stator and the rotor magnetic fields are at 90°. To sustain the running of the motor, the windings should be energized with respect to a particular squence considering position information and this is named as Commutation [10].

Figure 3 shows the back EMF and stator current waveforms besides electromagnetic power of bldc motor during commutation period. The electromagnetic power is obtained from summing of being multiplied with back EMFs and currents, shown in Equation (5) [18].

$$P_0 = e_a i_a + e_b i_b + e_c i_c \tag{5}$$

Electromagnetic power is written as kinetic energy form represented in [18] by neglecting the mechanical and stray losses, as the following equation;

$$P_0 = T_e \omega \tag{6}$$

where, T_e is electromagnetic torque and ω is angular velocity of rotor.

Substituting Equation (6) into Equation (5), the electromagnetic torrque is defined as;

$$T_e = \frac{(e_a i_a + e_b i_b + e_c i_c)}{\omega} \tag{7}$$

In order to constitute a consummate mathematical model of BLDC motor, the motion equation is written as;

$$T_e - T_L = J\frac{d\omega}{dt} + B_V\omega \quad (8)$$

where, T_L is load torque, J rotor moment of inertia and B_V is viscous friction coefficient.

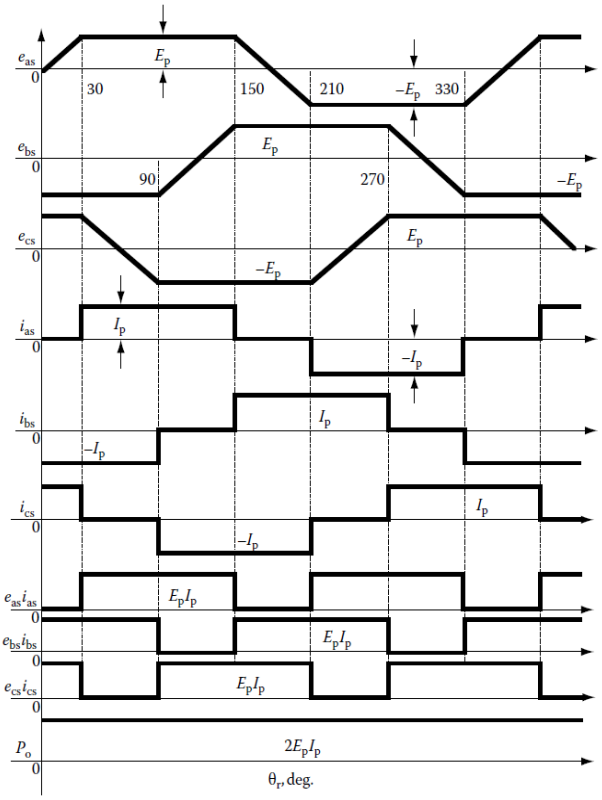

Figure 3. BLDC Motor Waveforms [13]

III. SPEED CONTROL WITH SENSOR AND SENSORLESS TECHNIQUES

The BLDC motor velocity control with a closed loop controller which is shown as block diagram in Figure 3., ensures the motor operation at any desired speed. By comparing the actual and reference speed values, an error signal is generated. The speed error signal is input for a speed regulatory mechanism, which is based on a Proportional-Integral (PI) controller which controls the velocity with appropriate proportional and integral gain values [11]. Reference torque is obtained at output of the PI controller. The reference torque is transformed to the reference current by using BLDC motor torque-current equation. Obtained reference current is compared with the actual measured stator current and the current error is sent to the input of hysteresis current controller to generate gate pulses [12]. Instantaneous control of the current is not realized by PWM controller. The hysteresis controller which converts voltage source to fast-acting current source is utilized to overcome this problem. Furthermore, the hysteresis controller is a very simple closed-loop control scheme and also it regulates the currents with a narrow band around the reference current by comparing the actual current [13, 14].

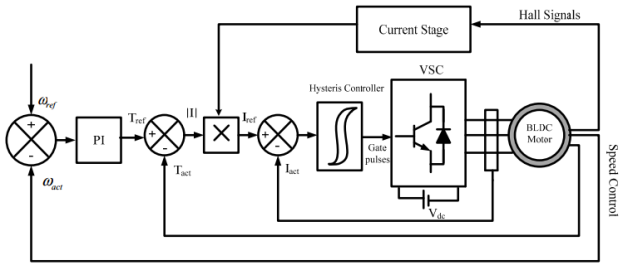

Figure 4. Closed loop velocity control of the BLDC motor [12]

In this study, aforementioned closed loop control technique has been used for controlling the speed of BLDC motor. Sliding mode observer technique and other two different methods which are hall sensor and the detection of zero crossing point of back EMF are evaluated severally in the next section.

A. Speed Control with Hall Sensor

In this control strategy, the rotor position data obtained from the sensors are used to turn on and off the switches as shown in Figure 5. Each interval of the current conduction is named as one step. Just only two of three phases are energized to provide flowing the current at any time, leaving third phase floating. The gates of the inverter should be triggerred at every 60° for commutation to produce maximum torque so that back EMF and current can be in the same phase [16].

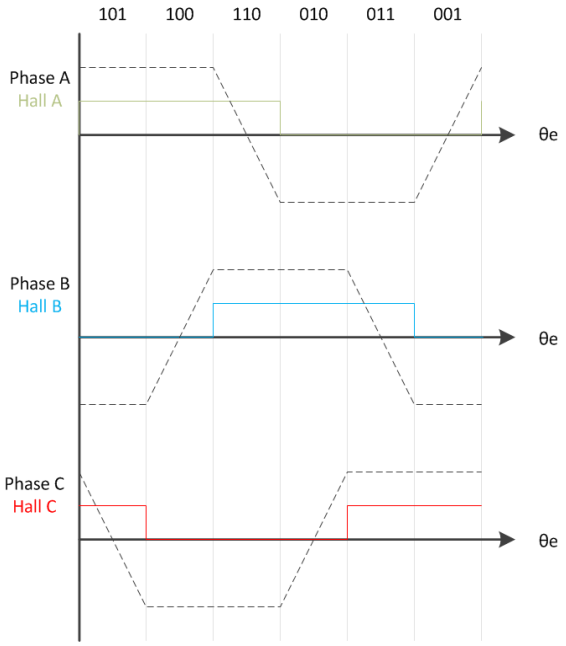

Figure 5. Hall Effect Signals with the back EMF signals [15]

Table 1. Switching Sequence [16]

Switching Interval	Sequence Number	Pos. Sensors			Switch Closed		Phase Current		
		H1	H2	H3			A	B	C
0°-60°	0	1	0	0	Q1	Q4	+	-	Off
60°-120°	1	1	1	0	Q1	Q6	+	Off	-
120°-180°	2	0	1	0	Q3	Q6	Off	+	-
180°-240°	3	0	1	1	Q3	Q2	-	+	Off
240°-300°	4	0	0	1	Q5	Q2	-	Off	+
300°-360°	5	1	0	1	Q5	Q4	Off	-	+

The inverter commutates the current as shown in Figure 2 using hall sensors output signals generated based on rotor position data. The switching sequence, the diretion of the current and hall sensor signals are shown in Table 1 [15].

B. Speed Control with Detection of Zero Crossing Points for Back EMF

This control strategy is based on catching the back EMF zero crossing points in floating phase, which is the simple method for back EMF sensing techniques. As illustrated in Figure 6, the commutation points can be predicted when the back EMF crosses zero point with a 30° phase shift [17]. As it mentioned before each phase conducts the current 120 electrical degrees and just two phases have conduction.

According to zero crossing points which are shifted 30°, virtual hall output signals are produced considering its positive cross point. In order to eliminate high frequency electromagnetic interferences and harmonics caused by gate switching in terminal voltages, low pass filters are used and as a result of this there is phase shifting of the signals at the same time. As shown in Figure 7, phase shift angle is calculated simply for the detected signals. For instance, as taking phase A in Figure 7, the relationship between real and processed signals, can be expressed as;

$$\frac{u'_A}{u_A}=\frac{R_2}{R_1+R_2+j2\pi fR_1R_2C_1} \tag{9}$$

where, f presents the back EMF frequency [17]. Phase delay is calculated as below,

$$\alpha=\arctan\frac{2\pi fR_1R_2C_1}{R_1+R_2} \tag{10}$$

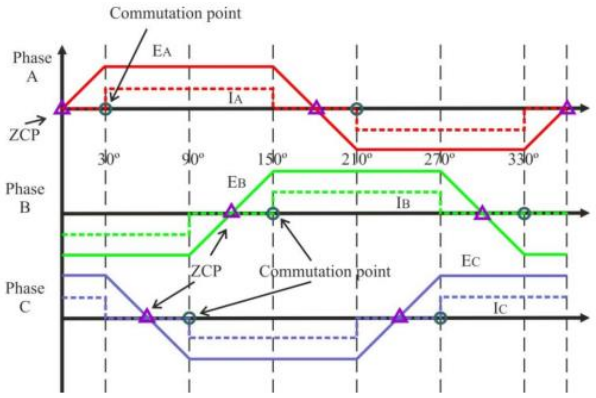

Figure 6. Back EMF zero crossing points and commutation points [17]

C. Speed Control with SMO Technique

This control method is utilized to estimate motor speed owing to good robustness and the antidisturbance ability for noise [18]. Sliding mode observer which generates a sliding action between the measured plant and the observer output is a reduced order current observer in which the terminal currents are the reference outputs and the adaptive model estimates motor currents. This ability ensures that a SMO produces estimations which are completely proportional with the output of the plant [19]. The BLDC motor could be modelled using below equations stated in [20] as considering all phases are stable.

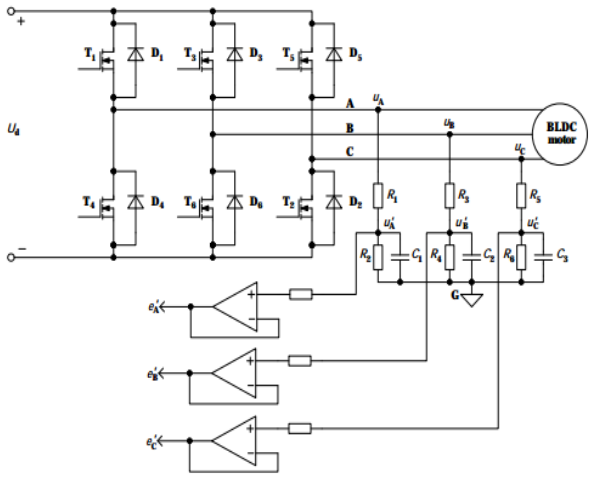

Figure 7. Back-EMF detection circuit [18]

$$\begin{aligned}
\frac{d}{dt}(i_a-i_b)&=-\frac{R}{L}(i_a-i_b)-\frac{1}{L}E_{ab}+\frac{1}{L}V_{ab}\\
\frac{d}{dt}(i_b-i_c)&=-\frac{R}{L}(i_b-i_c)-\frac{1}{L}E_{bc}+\frac{1}{L}V_{bc}\\
\frac{d}{dt}(i_c-i_a)&=-\frac{R}{L}(i_c-i_a)-\frac{1}{L}E_{ca}+\frac{1}{L}V_{ca}
\end{aligned} \tag{11}$$

where, E_{ab} , E_{bc} and E_{ca} are line to line back EMF, V_{ab} , V_{bc} and V_{ca} are line to line voltages, i_a , i_b , i_c are phase currents. When the sample period is chosen quite smaller than mechanical and electricial time constants, the changing between line to line back EMF during sampling periods are zero [20]. Therefore, equation (11) is again written as below;

$$\begin{aligned}
\frac{d}{dt}(i_a-i_b)&=-\frac{R}{L}(i_a-i_b)-\frac{1}{L}E_{ab}+\frac{1}{L}V_{ab}\\
\frac{d}{dt}(i_b-i_c)&=-\frac{R}{L}(i_b-i_c)-\frac{1}{L}E_{bc}+\frac{1}{L}V_{bc}\\
\frac{d}{dt}E_{ab}&=0\\
\frac{d}{dt}E_{bc}&=0
\end{aligned} \tag{12}$$

SMO, inspects the state variables according to convenient sliding face in system. The SMO predicts the line current and it is considered that the sliding face is between real and predicted line current in this platform. Equation (12) is transformed into SMO as:

$$\begin{aligned}
\dot{x}_1&=-\frac{R}{L}x_1-\frac{1}{L}\dot{x}_3+\frac{1}{L}V_{ab}+K_{11}\text{sign}(x_1-\dot{x}_1)\\
\dot{x}_2&=-\frac{R}{L}x_2-\frac{1}{L}\dot{x}_4+\frac{1}{L}V_{bc}+K_{22}\text{sign}(x_2-\dot{x}_2)\\
\dot{x}_3&=-K_{31}\text{sign}(x_1-\dot{x}_1)\\
\dot{x}_4&=-K_{41}\text{sign}(x_2-\dot{x}_2)
\end{aligned} \tag{13}$$

where, x_1 is the difference between line currents (a and b phases); x_2 is the difference between line currents (b and c phases); x_3 is the line to line back EMF for ab; x_4 is the line to line back EMF for bc; K_{11} and K_{22} are the current observer gain; K_{31} and K_{41} are back EMF observer gains. By setting $e=x-\hat{x}$, error dynamics are shown in (14):

$$\begin{aligned}\dot{e}_1 &= -\frac{1}{L}e_3 + K_{11}\text{sign}(e_1)\\ \dot{e}_2 &= -\frac{1}{L}e_4 + K_{22}\text{sign}(e_2)\\ \dot{e}_3 &= -K_{31}\text{sign}(e_1)\\ \dot{e}_4 &= -K_{41}\text{sign}(e_2)\end{aligned} \quad (14)$$

In conventional SMO technique, signum function is defined as mentioned in (10). This approachment has undesirable chattering which decreases the accuracy of rotor position data [20]. In order to eliminate this effect, equations in (14) are revised by saturation function in Equation (15):

$$\begin{aligned}\dot{e}_1 &= -\frac{1}{L}e_3 + K_{11}\text{sat}(e_1)\\ \dot{e}_2 &= -\frac{1}{L}e_4 + K_{22}\text{sat}(e_2)\\ \dot{e}_3 &= -K_{31}\text{sat}(e_1)\\ \dot{e}_4 &= -K_{41}\text{sat}(e_2)\end{aligned} \quad (15)$$

The signum and saturation functions formulated in [21] are defined as follows:

$$\text{sign}(e) = \begin{cases} 1; & e > 0 \\ 0; & e = 0 \\ -1; & e < 0 \end{cases} \quad (16)$$

$$\text{sat}(e) = \begin{cases} \frac{e}{\varepsilon}; & |e| \le \varepsilon \\ 0; & e = 0 \\ \text{sign}(e); & |e| > \varepsilon \end{cases} \quad (17)$$

where, ε is sliding surface band. The stability analysis is done by Lyapunov function referenced in [19] as follows:

$$S(e) = \frac{1}{2}\left(e_1^2 + e_2^2\right) \quad (18)$$

where, S is the sliding surface which is error between the actual and estimated currents. The derivative of *S(e)* according to time is as follow.

$$\begin{aligned}\dot{S}(e) &= e_1\dot{e}_1 + e_2\dot{e}_2\\ &= e_1\left[-\frac{1}{L}e_3 + K_{11}sat(e_1)\right] + e_2\left[-\frac{1}{L}e_4 + K_{22}sat(e_2)\right]\end{aligned} \quad (19)$$

Observer gains should be selected to satisfy the $S \cdot \dot{S} < 0$ limitation to keep SMO stabilization [19].

The proposed sensorless velocity control of the BLDC motor with SMO technique is illustrated in Figure 8. The back EMF is estimated with SMO by measuring line to line voltages and currents, and the rotor position is extracted using the speed which is transformed from the back EMF. In view of relationship between the back EMF and the speed, they are tranformed into each other. The variation of speed is utilized to predict the back EMF, therefore function of the estimated back EMF includes the estimation of speed in shown in Figure 9 [20]. This speed value is sent to the difference block in which output is error between actual and reference speed values.

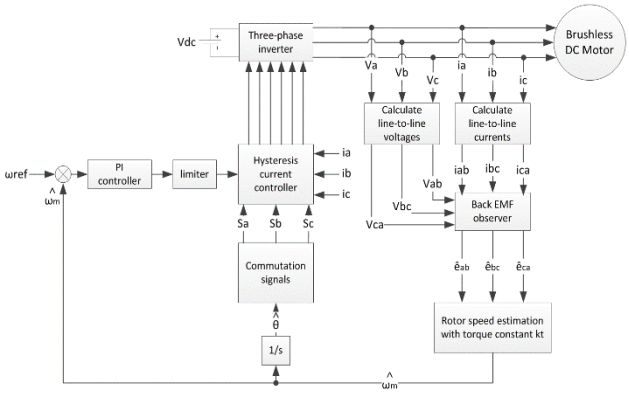

Figure 8. Proposed SMO speed control for BLDC motor

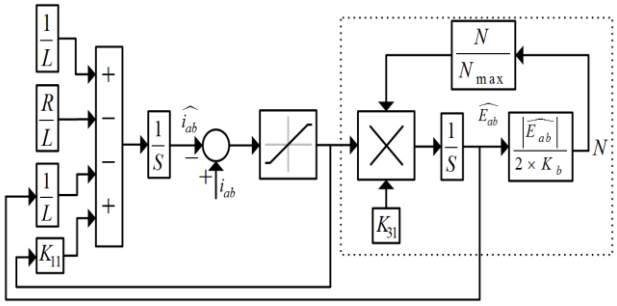

Figure 9. SMO technique with Sigmoid function [19]

IV. SIMULATION RESULTS

Three methods mentioned in previous section, are evaluated with respect to their simulation performance studied in MATLAB/Simulink environment in this section. The speed control of BLDC motor with these three methods is simulated and also BLDC motor, PI controller and SMO parameters are represented in Table 2. Simulation results are discussed for the BLDC motor with closed loop control runnig at fixed speed by changing the load.

Table 2. Motor parameters and PI controller parameters

Paremeters	Symbol	Numerical
Poles	p	4
Stator phase resistance	R_s	1.535 Ω
Stator phase inductance	L_s	3.285 mH
Torque constant	k_t	0.49 N.m/A
Moment of inertia	J	1.8e^{-4} kg.m^2
Friction coefficient	B	0.001 N.m.s
DC link voltage	V_{dc}	310 V
Rated Speed	ω_{rated}	4600 rpm
Rated Torque	T_{rated}	2.2 N.m
Rated Current	I_{rated}	4.52 A
k_p	0.0035	
k_i	0.136	
K_{11}	75000	
K_{31}	-19500000	

A. Case1: Hall Sensor Control

This model shown in Figure 10 based on hall sensors create three signals corresponding to position data with a phase shift of 120° to facilitate the control of the motor in a closed loop system. According to these three signals, the corresponding commutation switches are energized as

mentioned before in Table 1. The closed loop control system is used for regulating the current and the speed of the motor. The current error is sent to the hysteresis controller. The simulink results of the current and back EMF for phase "A" are shown in Figure 11 and the speed and torque waveforms of the motor are shown in Figure 12. Figures 13 and 14 show speed and electromagnetic torque under 2.2 N.m and 3 N.m instantaneous load conditions, respectively.

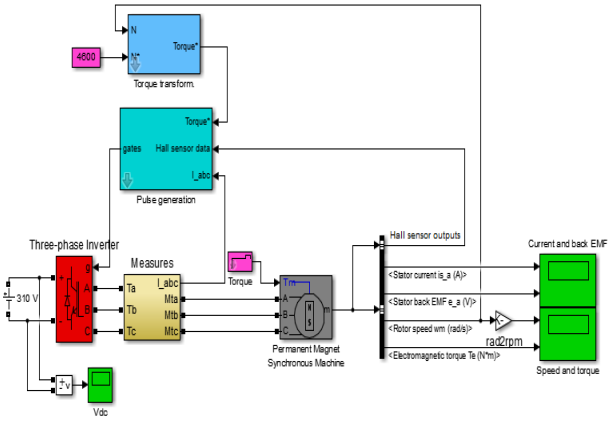

Figure 10. Simulation model of Hall sensor control

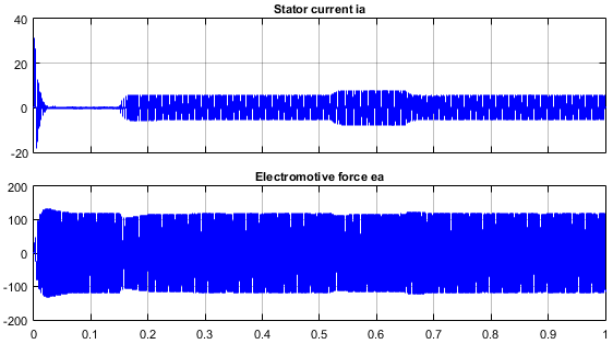

Figure 11. Results of the phase A current and back EMF with Hall sensor control

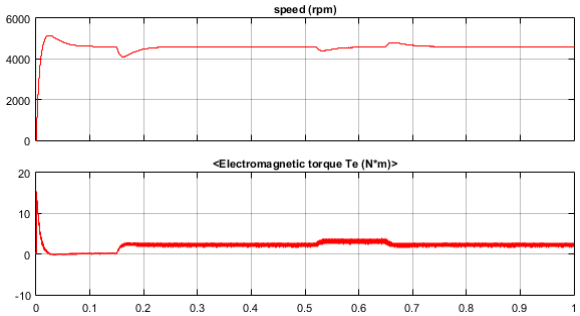

Figure 12. Results of speed and torque with Hall sensor control

B. Case 2: Back EMF Sensing Control

The model of direct back EMF sensing technique is shown in Figure 15. This model is based on the back EMF zero crossing points of floating phase. First of all, the back EMF is quite low for prediction of the position information of the rotor. Therefore, the motor needs to accelerate a convenient speed to detect the back EMF, so as to start the motor, an open loop starting is required until the speed is reached sufficient value. When the velocity of the motor is enough to detect the back EMF, the control mode is changed from open loop control to detection of the back EMF positive zero crossing points, which are shifted 30° by resistor and capacitor as shown in Figure 15. According to the detected positive points, virtual hall sensor outputs are produced as logical. These logical values represent the rotor position, also commutation points.

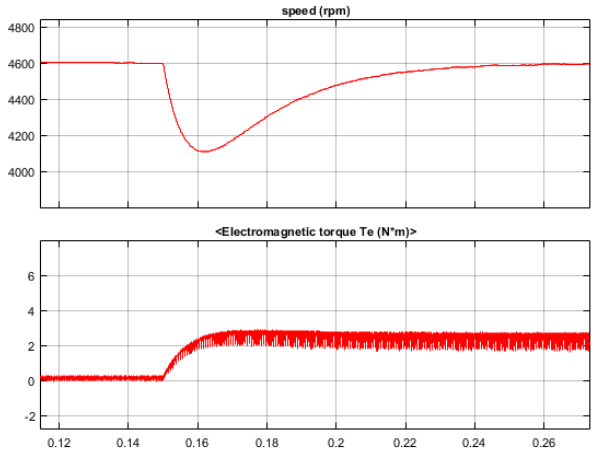

Figure 13. Results of speed and torque under 2.2 N.m load

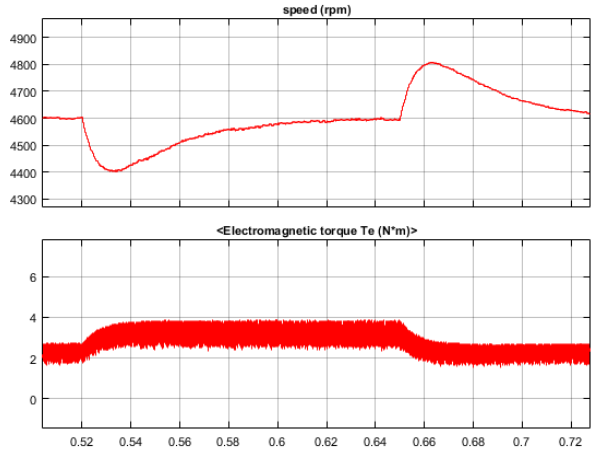

Figure 14. Results of speed and torque under instantaneous 3 N.m load

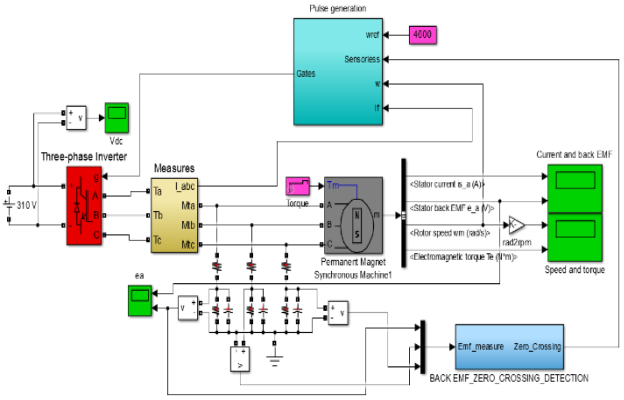

Figure 15. Simulation model of back EMF Detection

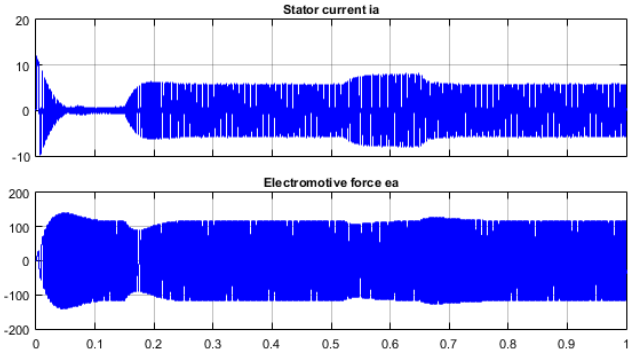

Figure 16. Results of the phase A current and back EMF waveform with back EMF detection

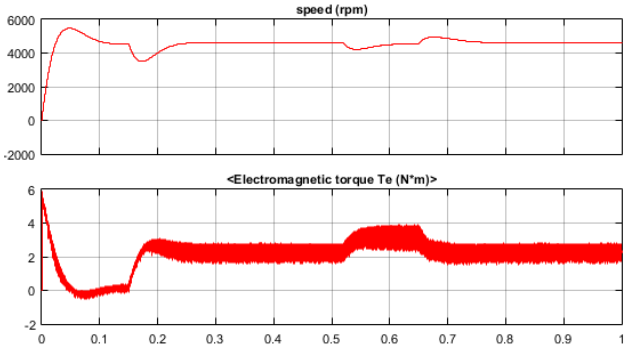

Figure 17. Results of speed and torque with back EMF Detection

As mentioned in Case 1, the same control techniques which are PI and Hysteresis controllers are used in this study, considering the determined logical values. The simulink results of the current and back EMF for phase "A" are shown in Figure 16 and the speed and torque waveforms of the motor are shown in Figure 17. Figures 18 and 19 show speed and electromagnetic torque under 2.2 N.m and 3 N.m instantaneous load conditions, respectively.

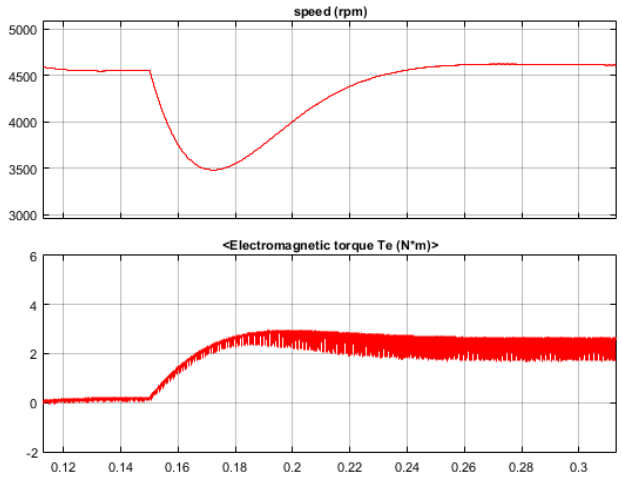

Figure 18. Simulation result of speed and torque under 2.2 N.m load

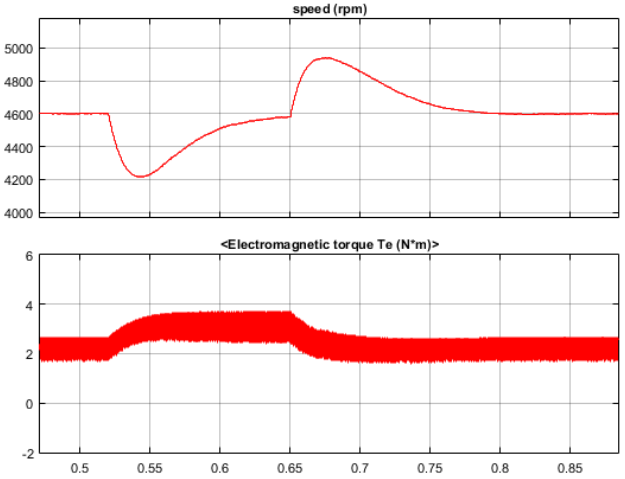

Figure 19. Results of speed and torque under instantaneous 3 N.m load

C. Case 3: Sliding Mode Observer (SMO) Control

The model of SMO control method is shown in Figure 20. This model is based on speed estimation with mathematical operations. Since the motor back EMF and speed are interrelated with each other, the speed is calculated by using the back EMF. The integration of the estimated speed gives the motor position angle which is used for detection three logical level as same as the output of Hall sensors. These three outputs are interpreted the firing signals of the gates which are switch on or off.

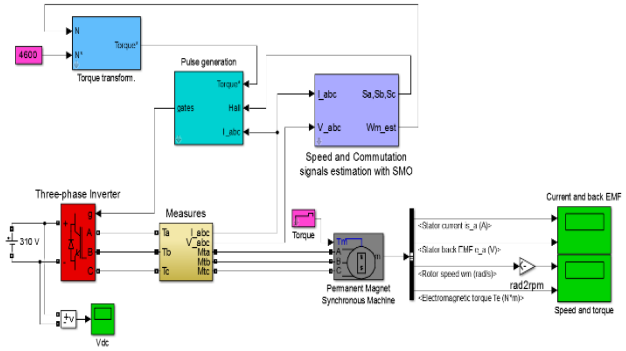

Figure 20. Simulation model of Sliding Mode Observer

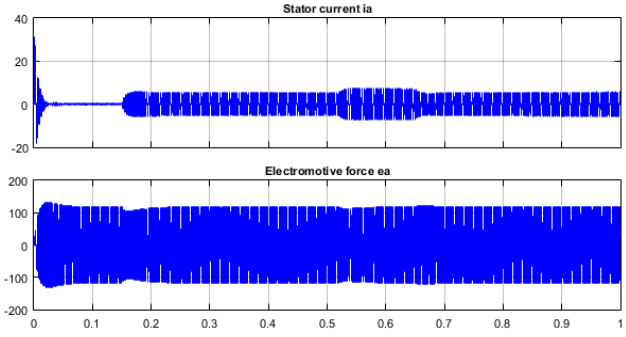

Figure 21. Results of the phase A current and back EMF with SMO

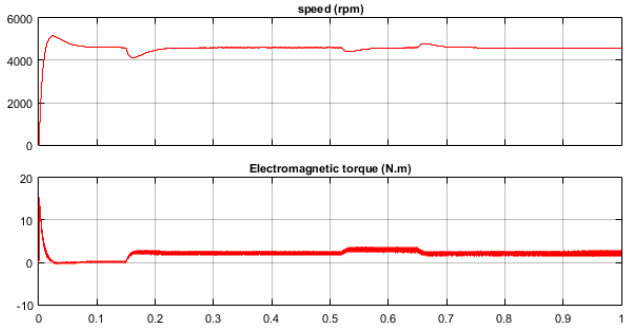

Figure 22. Results of speed and torque with SMO

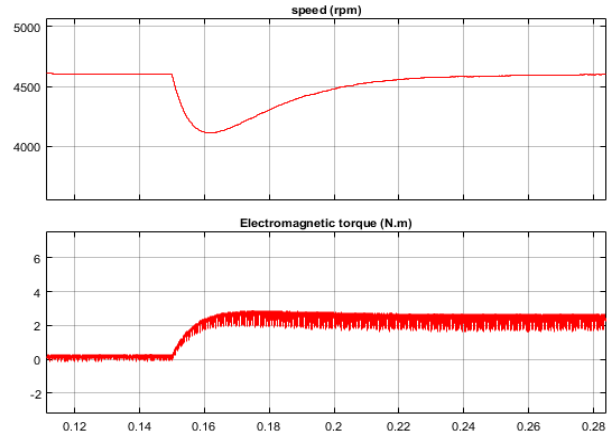

Figure 23. Simulation result of speed and torque under 2.2 N.m load

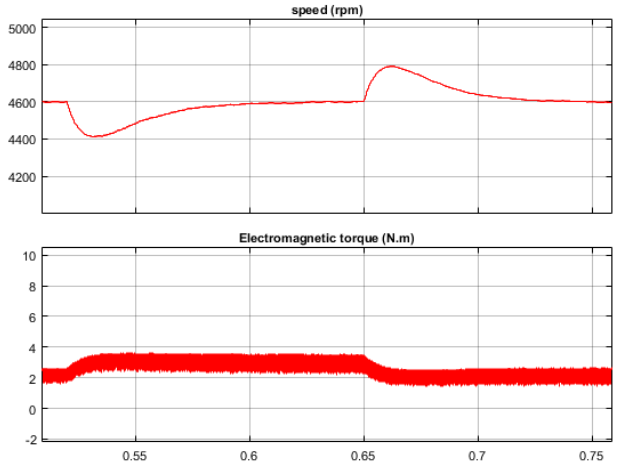

Figure 24. Results of speed and torque under instantaneous 3 N.m load

As mentioned in Case 1, the same control techniques which are PI and Hysteresis controllers are used in this study, considering the information of estimated rotor position. The simulink results of the current and back EMF for phase "A" are shown in Figure 21 and the speed and torque waveforms of the motor are shown in Figure 22. Figures 23 and 24 show speed and electromagnetic torque under 2.2 N.m and 3 N.m instantaneous load conditions, respectively.

V. CONCLUSIONS

The speed control of the BLDC motor is discussed using three different methods based on with-sensor and sensorless techinques. In hall sensor control, the motor position is directly known by sensor. In direct back EMF detection control, commutation instants are determined using the line voltages. Three motor terminal voltages need to measured and filtered in order to improve the signal quality and shift the phase. This technique is well suited for narrow velocity ranges because of filtering the line, also back EMF zero crossing points are not detected at standstill condition. It is required that the motor should accelerate until the back EMF is detectable value.

The last control technique, a sensorless control of BLDC motor using SMO is proposed. The SMO is designed to predict the position of rotor without any help of the sensors. The actual rotor position as well as the machine speed can be estimated strictly even in the transient load statement. This method presents a precise control for speed and a detection the rotor position effectively over a wide speed range. The PI controller is implemented to control velocity in all methods. Besides, hysteresis controller is used to control inverter for better performance of the motor with the help of terminal currents, speed and rotor position. In direct back EMF control, the speed falls below 3600 rpm when the 2.2 N.m load is applied, however, it is about 4000 rpm in the other two methods. Consequently, simulation results indicate that hall sensor and SMO control have almost the same performance and they are more precise by comparison with direct back EMF control.

REFERENCES

[1] P. Damodharan, K. Vasudevan., "Sensorless Brushless DC Motor Drive Based on the Zero-Crossing Detection of Back Electromotive Force (EMF) From the Line Voltage Difference", IEEE Trans. Energy Convers., Vol. 25, No. 3, pp. 661-668, Sep. 2010.

[2] R.M. Pindoriyal, A.K. Mishra, B.S. Rajpurohie, R. Kumar, "Analysis of Position and Speed Control of Sensorless BLDC Motor using Zero Crossing Back-EMF Technique", 1st IEEE International Conference on Power Electronics, Intelligent Control and Energy Systems, 2016.

[3] J. Shao, D. Nolan, M. Teissier, D. Swanson, "A Novel Microcontroller Based Sensorless Brushless DC (BLDC) Motor Drive for Automotive Fuel Pumps", IEEE Trans. Ind. Appl., Vol. 39, No. 6, pp. 1734-1740, Nov./Dec. 2003.

[4] P.R Ashish, G. Vincent, "Sensorless Control of BLDC Motor Using Third Harmonic Back EMF", International Journal of Industrial Electronics and Electrical Engineering, Vol. 2, Issue 1, 2014.

[5] G.J. Su, J.W. McKeever, "Low Cost Sensorless Control of Brushless DC Motors with Improved Speed Range", IEEE Trans. Power Electron., Vol. 19, No. 2, pp. 296-302, Mar. 2004.

[6] S. Ogasawara, K. Suzuki, H. Akagi, "A Sensorless Brushless DC Motor System", Electr. Eng. Jpn., Vol. 112, No. 5, pp. 109-18, 2007.

[7] T.S. Kim, B.G. Park, D.M. Lee, J.S. Ryu, D.S. Hyun, "A New Approach to Sensorless Control Method for Brushless DC Motors", International Journal of Control, Automation and Systems, Vol. 6, No. 4, pp. 477-487, August 2008.

[8] Ch.H. Yu, "A Practical Sensorless Commutation Method Based on Virtual Neutral Voltage for Brushless DC Motor", IEEJ Trans., pp. 770-77, 2017.
[9] M.H. Rashid, "Power Electronics Handbook", Departmant of Electrical and Computer Engineering, University of West Florida, 2007.
[10] P. Yedamale, "Brushless DC (BLDC) Motor Fundamentals", Microchip, Application Note, AN885, USA, 2003.
[11] H.K. Samitha Ransara, U.K. Madawala, "A Low Cost Drive for Three-Phase Operation of Brushless DC Motors", IECON Proceedings (Industrial Electronics Conference), 6119561, pp. 1692-1697, 2011.
[12] P. Sarala, S.F. Kodad, B. Sarvesh, "Analysis of Closed Loop Current controlled BLDC Motor Drive", International Conference on Electrical, Electronics, and Optimization Techniques (ICEEOT), pp. 1464-1468, 2016.
[13] R. Krishnan, "Permanent Magnet Synchronous and Brushless DC Motor Drives", Virginia Tech Blacksburg, Virginia, USA, 2010.
[14] M. Ebadpour, M.B.B. Sharifian, "Cost Effective Current Control and Commutation Torque Ripple Reduction in Brushless DC Motor Drives", International Journal on Technical and Physical Problems of Engineering (IJTPE), Issue 18, Vol. 6, No.1, pp. 154-159, March 2014.
[15] M. Johansson, "Evaluation of Sensor Solutions & Motor Speed Control Methods for BLDCM/PMSM in Aerospace Applications", Master Thesis, Lulea University of Technology, Sweden, 2017.
[16] J.E. Muralıdhar, P. Varanasi, "Torque Ripple Minimization & Closed Loop Speed Control of BLDC Motor with Hysteresis Current Controller", 2nd International Conference on Devices, Circuits and Systems (ICDCS), 2014.
[17] T. Kim, H.W. Lee, M. Ehsani, "Position SensorlessBrushless DC Motor/Generator Drives: Review and Future Trends", lET Elect. Power Appl., Vol. 1, pp. 557-564, 2007.
[18] C.L. Xia, "Permanent Magnet Brushless DC Motor Drives and Controls", John Wiley & Sons Singapore Pte. Ltd., 2012.
[19] M.R. Feyzi, M. Shafiei, "Position Sensorless Direct Torque Control of Brushless DC Motor Drives Based on Sliding Mode Observer Using NSGA-II Algorithm Optimization", 2nd Power Electronics, Drive Systems and Technologies Conference, pp. 151-156, 2011.
[20] A. Deenadayalan, G. Saravana Ilango, "Modified Sliding Mode Observer for Position and Speed Estimations in Brushless DC Motor", IEEE INDICON, India, pp. 1-4, 2011.
[21] P.K. Girija, A. Prince, "Robustness Evaluation of SMO in Sensorless Control of BLDC Motor under DTC Scheme" International Conference on Power, Signals, Control and Computation, EPSCICON, 2014.

BIOGRAPHIES

Mustafa Topal was born in Merzifon, Turkey, in 1988. He received the B. Eng. degree in electrical and electronics engineering from Erciyes University, Kayseri, Turkey in 2013. He presently studies M. Eng. degree in electrical and electronics engineering in Gazi University, Ankara, Turkey. His research interests include permanent-magnet dc motor control and power electronics.

Ires Iskender received the B.Sc. degree in Electrical and Electronics Engineering from Gazi University (Ankara, Turkey) in 1987. He acquired his M.Sc. and Ph.D. degrees in Electrical and Electronics Engineering from Middle East Technical University (Ankara, Turkey) in 1990 and 1996, respectively. Prior to joining Department of Electrical and Electronics Engineering, Cankaya University (Ankara, Turkey), he worked at Department of Electrical and Electronics Engineering in Middle East Technical University, and Gazi University. His current research interests are energy conversion systems, renewable energy sources, electrical machine, and power quality. He participated in and coordinated several research projects and he served as the panelist and referee for many academic or industry projects.

Naci Genc received the B.Sc., M.Sc., and Ph.D. degrees from Gazi University (Ankara, Turkey), Van Yuzuncu Yil University (Van, Turkey) and Gazi University in 1999, 2002, and 2010, respectively. He is a Professor in the Electrical and Van Yuzuncu Yil University. His interests include energy conversion systems, power electronics and electrical machines.